AIP | APL Materials

Transparent ferrimagnetic semiconducting $CuCr_2O_4$ thin films by atomic layer deposition

T. S. Tripathi, C. S. Yadav, and M. Karppinen

Citation: APL Mater. **4**, 046106 (2016); doi: 10.1063/1.4946884
View online: http://dx.doi.org/10.1063/1.4946884
View Table of Contents: http://scitation.aip.org/content/aip/journal/aplmater/4/4?ver=pdfcov
Published by the AIP Publishing

Transparent ferrimagnetic semiconducting $CuCr_2O_4$ thin films by atomic layer deposition

T. S. Tripathi,[1] C. S. Yadav,[2] and M. Karppinen[1,a]
[1]*Department of Chemistry, Aalto University, P.O. Box 16100, FI-00076 Aalto, Finland*
[2]*School of Basic Sciences, Indian Institute of Technology Mandi, Mandi, H.P. 175001, India*

(Received 27 February 2016; accepted 4 April 2016; published online 14 April 2016)

We report the magnetic and optical properties of $CuCr_2O_4$ thin films fabricated by atomic layer deposition (ALD) from $Cu(thd)_2$, $Cr(acac)_3$, and ozone; we deposit 200 nm thick films and anneal them at 700 °C in oxygen atmosphere to crystallize the spinel phase. A ferrimagnetic transition at 140 K and a direct bandgap of 1.36 eV are determined for the films from magnetic and UV-vis spectrophotometric measurements. Electrical transport measurements confirm the p-type semiconducting behavior of the films. As the ALD technique allows the deposition of conformal pin-hole-free coatings on complex 3D surfaces, our $CuCr_2O_4$ films are interesting material candidates for various frontier applications.
[http://dx.doi.org/10.1063/1.4946884]

Atomic layer deposition (ALD) is a state-of-the-art thin-film deposition technique particularly advantageous to applications where precisely thickness-controlled and pin-hole-free nanoscale coatings are required on high-aspect-ratio substrates. The unique atomic layer-by-layer growth mechanism via self-saturative surface reactions makes it attractive for the fabrication of modern semiconducting devices with complex 3D architectures.[1–4] Here, we use the technique to deposit high-quality transparent semiconducting p-type $CuCr_2O_4$ thin films. Spinel-structured chromium oxides ACr_2O_4 (A = Cu, Mn, Fe, Co, and Ni) exhibit a wide range of electronic, magnetic, and optical properties through the variation of the A-site cation constituent.

At high temperatures, the ACr_2O_4 compounds possess the normal cubic spinel structure with space group $Fd\bar{3}m$. Within this structure, cations on the A and B sites form a bipartite lattice system. The A^{2+} cations sit on the tetrahedral sites in a diamond sublattice formed by the oxygen atoms, while the octahedrally coordinated B-site Cr^{3+} cations form a pyrochlore-type sublattice with edge-sharing oxygen octahedra.[5] The nature and the type of intra- and/or inter-site interactions between the A- and B-site cations are then the main source of various exotic ground states in this material family.[6,7] In particular, the strong preference of Cr^{3+} cations towards octahedral coordination minimizes the cation site disorder in ACr_2O_4 spinels. They are thus ferrimagnetic in nature and have been identified as, e.g., novel spin filter materials for magnetic junctions.[8,9] Most importantly, it has been observed that the isostructural interface between half-metallic Fe_3O_4 electrodes and the spinel barrier layer gives rise to a significant increase in junction magnetoresistance that surpasses the values previously reported for Fe_3O_4-based junctions. Very recently, an optical resistive switching behavior was reported for the A = Cu member of the ACr_2O_4 family in Ag/$CuCr_2O_4$/FTO devices.[10] Besides, the same $CuCr_2O_4$ phase with the unique tetragonally distorted normal spinel structure with $c/a < 1$[11] has also been highlighted as a prominent catalyst in, e.g., various oxidation, hydrogenation, and alkylation reactions of large-scale industrial relevance.[12–14] A more recent application area is the solid oxide fuel cell where spinel oxides including $CuCr_2O_4$ are being explored

[a]maarit.karppinen@aalto.fi

as interconnect materials that need to show both high corrosion resistance and high electrical conductivity.[15] Moreover, $CuCr_2O_4$ and related materials have found usable as burn rate modifiers in solid propellant processing for space launch vehicles.[16–18] The various application possibilities and corresponding fabrication challenges were recently summarized in the review article of Prasad and Singh,[19] underlining the importance of further endeavors to explore $CuCr_2O_4$ for its improved functionalities.

Normally, the spinel oxides are insulating in nature due to their prevailing ionic bonding. However, there are few unambiguous reports regarding the electrical conductivity of $CuCr_2O_4$.[14,20] In some reports, it has been found to be an insulator while in others a p-type narrow-bandgap semiconductor.[21] Magnetically, it is ferrimagnetic and crystal structure-wise a tetragonally distorted (a = b = 6.03 Å, c = 7.78 Å, c/a = 1.29) normal spinel at room temperature.[22,23] The tetragonal distortion is a consequence of the Jahn–Teller effect of Cu^{2+} cations that removes the ground-state degeneracy resulting in the flattening of the CuO_4 tetrahedra to the lower-symmetry tetragonal phase. However, upon heating, it transforms to the cubic spinel phase near 600 °C, where the compression of the CuO_4 tetrahedra is removed by orbital melting (transition from an orbital-ordered to orbital-disordered state).[24]

There are very few thin-film studies for $CuCr_2O_4$. An enhanced magnetization in excess of 200% of the accepted bulk value was reported due to substrate strain for pulsed laser deposited (PLD) epitaxial $CuCr_2O_4$ thin films on single-crystal (110) $MgAl_2O_4$ substrates.[25] The spin-coating method was employed for depositing $CuCr_2O_4$ films for resistive switching[10] and the phase was also found as a co-product in some rf-sputtered Cu–Cr–O films.[26–28] There is one report where the metal organic chemical vapor deposition (MOCVD) technique was used, with copper and chromium acetyl acetonate as precursors.[29] To the best of our knowledge, there are no ALD processes reported for this compound. Motivated by its attractive basic physical properties relevant to frontier applications where the ALD technology could be expected to be highly beneficial, we decided to develop an ALD process for $CuCr_2O_4$ and characterize the resultant thin films for their basic magnetic, optical, and electrical transport properties. As a starting point for the work, we utilize the detailed ALD growth parameters we recently optimized for the deposition of delafossite $CuCrO_2$ thin films.[30]

For the deposition of $CuCr_2O_4$ thin films, copper 2,2,6,6-tetramethyl-3,5-heptanedionate ($Cu(thd)_2$) and chromium acetyl acetonate ($Cr(acac)_3$) were used as metal precursors and ozone as the oxygen source; the depositions were carried out in a commercial hot-wall flow-type F-120 ALD reactor (ASM Microchemistry Ltd., Finland). The reactor was operated under a nitrogen (99.9995%) pressure of 2–3 mbar produced with a NITROX UHPN 3000 nitrogen generator. Nitrogen gas was used both as a carrier and purging gas. For the depositions, $Cu(thd)_2$ was prepared in-house from copper acetate (Fluka; 98%) and 2,2,6,6-tetramethyl hepatane-3,5-dione (Fluka; >98%), whereas for $Cr(acac)_3$ (97.5%) commercial powder (STREM Chemicals) was used. Ozone was produced from oxygen (99.999%; Fischer model 502 laboratory ozone generator) and pulsed into the reactor through a needle valve and a solenoid valve from the main ozone flow line.

The sublimation temperatures of the metal precursors, $Cu(thd)_2$ and $Cr(acac)_3$, were 120 and 130 °C, respectively;[30] the precursors were sublimed from open glass boats held inside the reactor. The pulse times were fixed at 2 s for all the three precursors (two metal precursors and ozone), followed by a 3 s long N_2 purge based on our work on delafossite $CuCrO_2$ films,[30] and all the depositions were carried out at 250 °C. To adjust the film composition to the desired copper and chromium molar ratio of 1:2, the following super-cycle sequence was optimized: $(Cu(thd)_2 + O_3) + 4 \times (Cr(acac)_3 + O_3)$. The correct elemental composition of the films was confirmed using wavelength-dispersive X-ray fluorescence spectroscopy (WD-XRF; PANanalytical Axios^{mAX} microanalysis system equipped with SST-mAX X-ray tube that virtually eliminates instrument drift). The aforementioned super-cycle was then repeated 300 times to yield $CuCr_2O_4$ films with the desired thickness of ca. 200 nm, i.e., with the growth rate of 0.67 nm per super-cycle. It is commonly observed for ALD-grown ternary oxides[31–34] that the as-deposited films are amorphous, and a post-deposition annealing is required for crystallization. The present films were annealed at 700 °C in a rapid thermal annealing (RTA) furnace (PEO 601; ATV Technologie GmbH) in an oxygen gas flow.

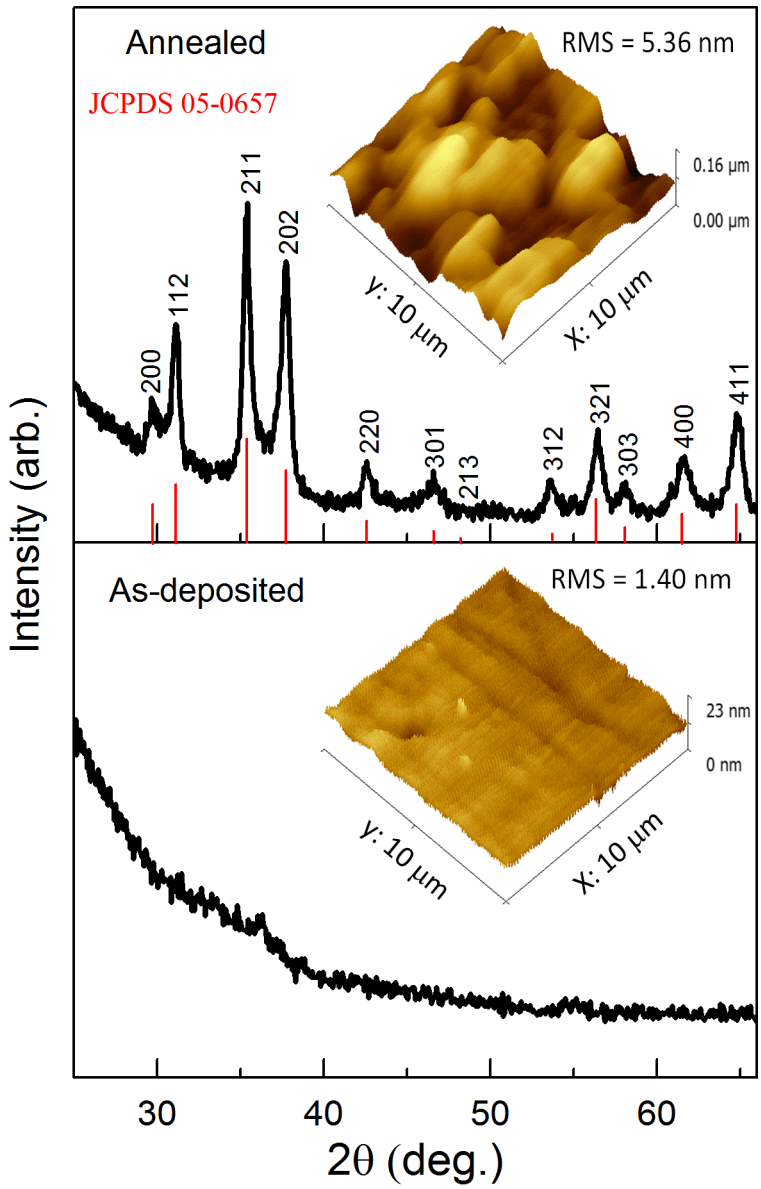

FIG. 1. GIXRD patterns and AFM images for as-deposited and annealed $CuCr_2O_4$ films. The red lines show the diffraction peaks matched with JCPDS reference data for $CuCr_2O_4$.

The films were deposited on borosilicate glass as the substrate material to allow the electrical transport and optical measurements. The UV-vis spectrophotometric measurements were carried out in the wavelength range of 190–1100 nm (Hitachi-U 2000 spectrophotometer). Grazing incidence X-ray diffraction measurement (GIXRD; PANalytical model X'pert Pro diffractometer, Cu Kα radiation) was performed to identify the crystal structure of the post-deposition annealed films. The same diffractometer was used for the thickness and density determination of the as-deposited thin films from X-ray reflectivity (XRR) patterns. The thickness of the films after annealing was confirmed from the cantilever tip jump using an atomic force microscope (AFM; TopoMetrix Explorer).[35] It should be noted that within the estimated error limits (<5%), the thickness of the films remained the same. For the physical property measurements, we deposited ca. 200 nm thick films. The structural parameters such as grain size (D) and dislocation density (δ) were calculated from the GIXRD patterns. The grain size of the thin films was calculated using Debye Scherrer's formula, $D = 0.9\lambda/\beta \cos\theta$, where D is the grain size, λ is the X-ray wavelength used, β

is the full width at half-maximum (FWHM) intensity in radians, and θ is Bragg's angle. Additionally, the dislocation density (δ) was evaluated by the formula,[36] $\delta = 1/D^2$, where the larger D and smaller δ values indicate better crystallization of the films. The surface topography and root-mean-square (RMS) roughness measurements were performed using the same atomic force microscope. Magnetic measurements were performed with DynaCool physical property measurement system (PPMS) from Quantum design equipped with vibration sample magnetometer (VSM). The specimen dimension was 10×5 mm^2.

In Figure 1, we show the GIXRD patterns for both as-deposited and O_2-annealed films. The as-deposited film is amorphous but, as expected, crystallizes upon the O_2-annealing at 700 °C. The annealing temperature 700 °C was chosen based on literature data revealing that the pure $CuCr_2O_4$ phase is formed above 450 °C, the degree of crystallinity enhancing with increasing temperature.[37] All the peaks in the GIXRD pattern can be readily indexed according to the spinel $CuCr_2O_4$ structure (JCPDS 05-0657). It is to be mentioned here that we have tried annealing the films in Ar atmosphere also but the resultant films had mixed phases of $CuCr_2O_4$ and $CuCrO_2$. The grain size estimated using the FWHM of the (211) peak at $2\theta \approx 35.16$ is ca. 30 nm. The dislocation density estimated for our $CuCr_2O_4$ films is 0.001 nm^{-2}.

We also took AFM images to demonstrate the changes in surface topography and RMS roughness upon the post-deposition annealing of our $CuCr_2O_4$ thin films, see Figure 1. Congruent to the GIXRD data, the RMS roughness value of 1.40 nm for the as-deposited film was found to increase to 5.36 nm for the annealed crystalline film; this trend is common for many ALD-grown amorphous films, which are extremely smooth after deposition and then upon the post-deposition heat treatment crystallize and become rougher.

To confirm the ferrimagnetic phase transition reported in literature for $CuCr_2O_4$, we measured the temperature dependence of magnetization at a magnetic field of 20 kOe for our crystalline $CuCr_2O_4$ thin film, see Figure 2. The data indicate that the Curie temperature (T_C) is approximately 140 K, which is in close agreement with the T_C values reported for epitaxial film[25] and bulk powder sample[23] of $CuCr_2O_4$. In the inset of Figure 2, we plot the magnetic hysteresis data measured at 10 K (after subtracting the diamagnetic contribution from the substrate). An average saturation magnetic moment of 0.28 μ_B/f.u. was estimated from the data using the calculated density 3.9 g/cc from the XRR fittings. The calculated density is, however, lower than the value of 5.4 g/cc reported in literature for bulk samples.[38] The estimated saturation magnetization of 0.28 μ_B/f.u is less than the values of 0.50[39] and 0.725 μ_B/f.u[40] reported in literature for single-crystal samples.

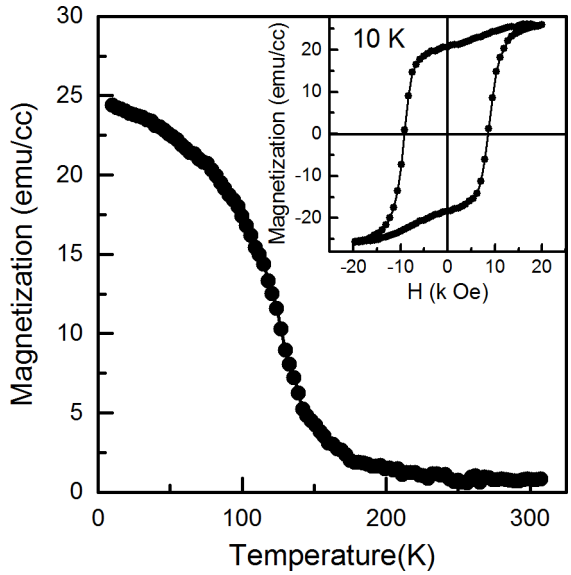

FIG. 2. Temperature dependence of magnetization measured for an annealed $CuCr_2O_4$ film in an applied magnetic field of 20 kOe; the inset shows the hysteresis loop at 10 K.

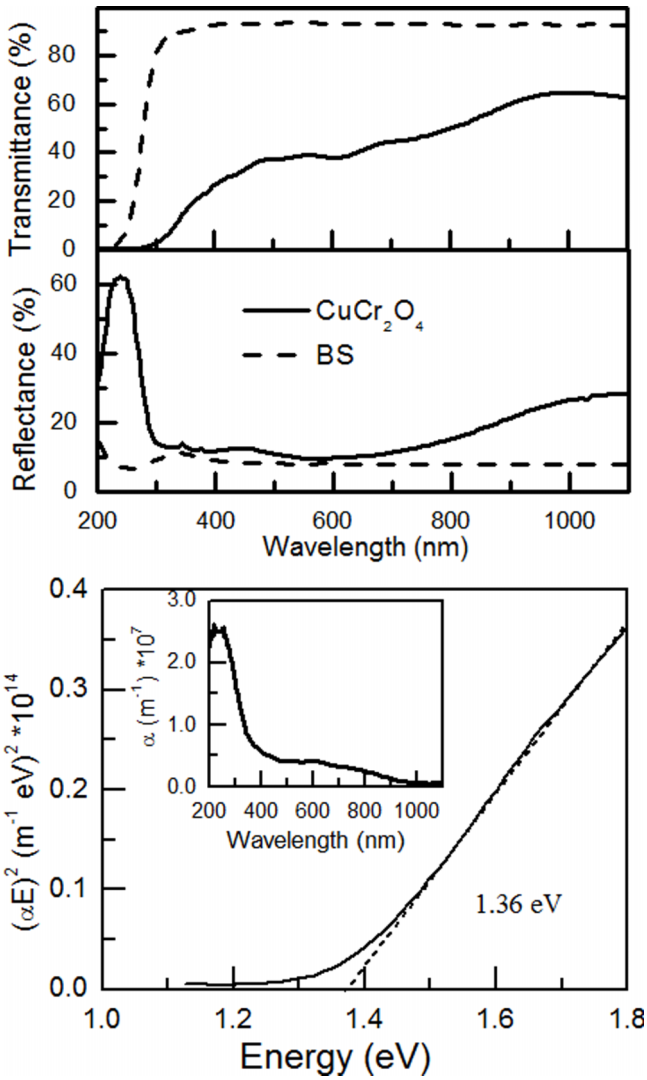

FIG. 3. UV-vis spectra measured as transmittance and reflectance for an annealed $CuCr_2O_4$ film and for the borosilicate substrate for reference; the lower panel demonstrates the determination of the direct energy bandgap. The inset shows the absorption coefficient as a function of wavelength.

The discrepancy in saturation moments may be related to complex non-collinear[23,39,40] nature of the magnetic structure with increased tetragonality due to an increase in the angle between the Cr^{3+}–Cr^{3+} spins. The increased angle results in decreased collinear projection along the Cu^{2+} spins, yielding the decreased net moment.[25]

In Figure 3, we present UV-vis spectra measured for the crystalline $CuCr_2O_4$ film. High transmittance (>60%) is observed in the wavelength range 800–1000 nm. As for the bandgap of $CuCr_2O_4$, there are very few reports in literature.[21] The bandgap and the absorption coefficient (α) at each wavelength have been calculated as reported by us in Ref. 30. The bandgap energy is then obtained as shown in the lower panel of Figure 3. The estimated bandgap 1.36 eV is in good agreement with values recently reported by Bajaj *et al.*[21] for $BiVO_4/CuCr_2O_4$ composites.

Finally in Figure 4, we show the Seebeck coefficient (S) and electrical resistivity (ρ) data for $CuCr_2O_4$. The p-type conductivity and the semiconducting-type behavior with temperature are seen from the positive Seebeck values and the negative $d\rho/dT$ slope, respectively. The inset shows the well-known exponential law between resistivity and temperature

$$\rho = \rho_0 \exp(\Delta E/k_B T), \quad (1)$$

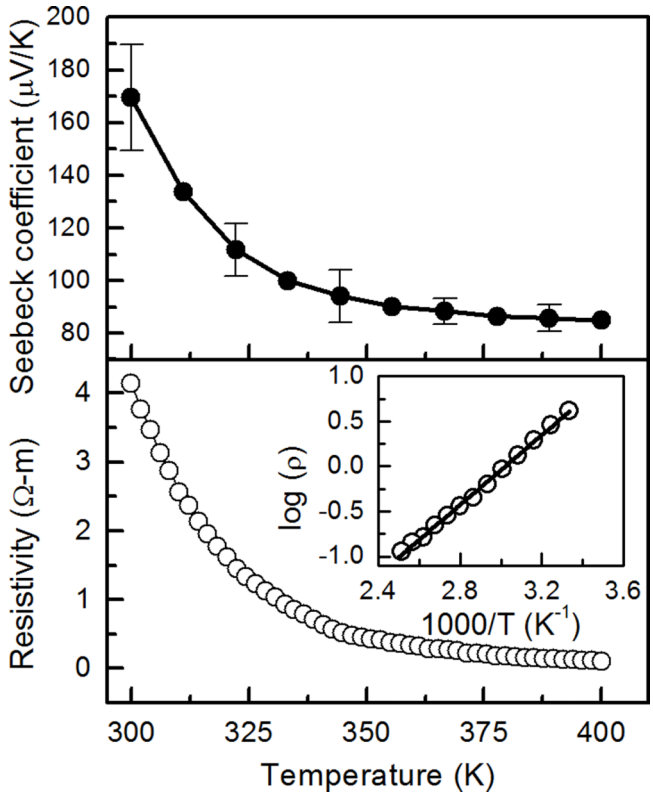

FIG. 4. Electrical transport properties measured as Seebeck coefficient and electrical resistivity as a function of temperature. The inset shows the log ρ vs 1/T plot for the calculation of electrical bandgap or activation energy.

where ρ is resistivity, ρ_0 is constant, ΔE is bandgap or activation energy, k_B is Boltzmann constant, and T is absolute temperature. The relation is obeyed strictly in the measured temperature range, which confirms the intrinsic semiconducting nature of the film. The value of ΔE = 0.17 eV is in good agreement with values reported for similar oxide spinels in literature.[41]

In the present work, we introduced an ALD process to fabricate $CuCr_2O_4$ thin films based on $Cu(thd)_2$, $Cr(acac)_3$, and ozone precursors. The as-deposited films were extremely smooth but amorphous. When annealed at 700 °C in O_2 then pure crystalline $CuCr_2O_4$ films were obtained with high transmittance values greater than 60% in the visible range with a direct bandgap of 1.36 eV. Magnetic measurements confirmed the ferrimagnetic phase transition with T_C close to 140 K. The estimated average saturation moment of 0.36 μ_B/f.u. is in good agreement with the value reported in literature for single crystal samples. Electrical transport measurements confirmed the p-type semiconducting behavior of the films.

The present work has received funding from the European Research Council under the European Union's Seventh Framework Programme (No. FP/2007-2013)/ERC Advanced Grant Agreement (No. 339478) and also from the Aalto Energy Efficiency Research Programme.

[1] *Atomic Layer Deposition for Semiconductors*, edited by C. Seong Hwang (Springer Science & Business Media, 2013).
[2] S. M. George, Chem. Rev. **110**, 111–131 (2010).
[3] R. W. Johnson, A. Hultqvist, and S. F. Bent, Mater. Today **17**, 236 (2014).
[4] F. Gao, S. Arpiainen, and R. L. Puurunen, J. Vac. Sci. Technol., A **33**, 010601 (2015).
[5] V. Kocsis, S. Bordács, D. Varjas, K. Penc, A. Abouelsayed, C. A. Kuntscher, K. Ohgushi, Y. Tokura, and I. Kézsmárki, Phys. Rev. B **87**, 064416 (2013).
[6] *Handbook of Magnetic Materials*, edited by E. P. Wohlfarth (North-Holland Publishing Company, 1982), Vol. 3.
[7] M. C. Kemei, S. L. Moffitt, L. E. Darago, R. Seshadri, M. R. Suchomel, D. P. Shoemaker, K. Page, and J. Siewenie, Phys. Rev. B **89**, 174410 (2014).
[8] G. Hu and Y. Suzuki, Phys. Rev. Lett. **89**, 276601 (2002).
[9] M. G. Chapline and S. X. Wang, Phys. Rev. B **74**, 014418 (2006).
[10] B. Sun, J. Wu, X. Jia, F. Lou, and P. Chen, J. Sol-Gel Sci. Technol. **75**, 664–669 (2015).

[11] P. S. Sathiskumar, C. R. Thomas, and G. Madras, Ind. Eng. Chem. Res. **51**, 10108–10116 (2012).
[12] H. Adkins and R. Connor, J. Am. Chem. Soc. **53**, 1091–1095 (1931).
[13] R. Connor, K. Folkers, and H. Adkins, J. Am. Chem. Soc. **54**, 1138–1145 (1932).
[14] S. Roy and J. Ghose, Mater. Res. Bull. **34**, 1179–1186 (1999).
[15] A. Petric and H. Ling, J. Am. Ceram. Soc. **90**, 1515 (2007).
[16] A. M. Kawamoto, L. C. Pardini, and C. Rezende, Aerosp. Sci. Technol. **8**, 591–598 (2004).
[17] P. W. M. Jacobs and H. M. Whitehead, Chem. Rev. **69**, 551–590 (1969).
[18] R. W. Armstrong, B. Baschung, and D. W. Booth, Nano Lett. **3**, 253–255 (2003).
[19] R. Prasad and P. Singh, Bull. Chem. React. Eng. Catal. **6**(2), 63 (2011).
[20] K. S. De, J. Ghose, and K. S. R. C. Murthy, J. Solid State Chem. **43**, 261 (1982).
[21] R. Bajaj, M. Sharma, and D. Bahadur, Dalton Trans. **42**, 6736–6744 (2013).
[22] N. Padmanaban, B. N. Avasthi, and J. Ghose, J. Solid State Chem. **81**, 250 (1989).
[23] E. Prince, Acta Crystallogr. **10**, 554 (1957).
[24] B. J. Kennedy and Q. Zhou, J. Solid State Chem. **181**, 2227 (2008).
[25] J. M. Iwata, R. V. Chopdekar, F. J. Wong, B. B. Nelson-Cheeseman, E. Arenholz, and Y. Suzuki, J. Appl. Phys. **105**, 07A905 (2009).
[26] R. S. Yu and C. M. Wu, Appl. Surf. Sci. **282**, 92–97 (2013).
[27] H. Sun, M. A. P. Yazdi, P. Briois, J. F. Pierson, F. Sanchette, and A. Billard, Vacuum **114**, 101–107 (2015).
[28] A. Barnabé, Y. Thimont, M. Lalanne, L. Presmanes, and P. Tailhades, J. Mater. Chem. C **3**, 6012–6024 (2015).
[29] Y. Chang, C. Lin, and B. Lee, in *ECS Proceedings of the Electrochemical Society 203rd Meeting - CVD XVI and EUROCVD 14*, edited by M. Allendorf, F. Maury, and F. Teyssandier (Electrochemical Society, Pennington, NJ, 2003), pp. 1492–1499.
[30] T. S. Tripathi, J.-P. Niemelä, and M. Karppinen, J. Mater. Chem. C **3**, 8364–8371 (2015).
[31] E. Ahvenniemi, M. Matvejeff, and M. Karppinen, Dalton Trans. **44**, 8001 (2015).
[32] K. Uusi-Esko, E.-L. Rautama, M. Laitinen, T. Sajavaara, and M. Karppinen, Chem. Mater. **22**, 6297–6300 (2010).
[33] K. Uusi-Esko and M. Karppinen, Chem. Mater. **23**, 1835–1840 (2011).
[34] M. Lie, O. Nilsen, H. Fjellvåg, and A. Kjekshus, Dalton Trans. **3**, 481 (2009).
[35] L. K. Tan, B. Liu, J. H. Teng, S. Guo, H. Y. Lowd, and K. P. Loh, Nanoscale **6**, 10584 (2014).
[36] W. D. Callister, *Materials Science and Engineering—An Introduction* (John Wiley and Sons, New York, 1997).
[37] Z. Ma, Z. Xiao, J. A. van Bokhoven, and C. Liang, J. Mater. Chem. **20**, 755–760 (2010).
[38] *Handbook of Inorganic Compounds*, 2nd ed., edited by D. L. Perry (CRC Press, 2011).
[39] K. Ohgushi, Y. Okimoto, T. Ogasawara, S. Miyasaka, and Y. Tokura, J. Phys. Soc. Jpn. **77**, 034713 (2008).
[40] M. R. Suchomel, D. P. Shoemaker, and L. Ribaud, Phys. Rev. B **86**, 054406 (2012).
[41] S. T. Kshirsagar and C. D. Sabane, Jpn. J. Appl. Phys., Part 1 **10**, 794 (1971).